

Phosphine-Catalyzed Domino Regio- and Stereo-Selective Hexamerization of 2-(Bromomethyl)acrylates to 1,2-Bis(cyclohexenyl)ethenyl Derivatives

Marta Papis, Raffaella Bucci, Alessandro Contini, Maria Luisa Gelmi, Leonardo Lo Presti, Giovanni Poli, Gianluigi Broggin, and Camilla Loro*



Cite This: *Org. Lett.* 2023, 25, 7380–7384



Read Online

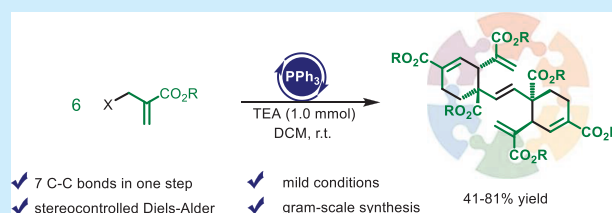
ACCESS |

Metrics & More

Article Recommendations

Supporting Information

ABSTRACT: A phosphine-catalyzed domino assembly of six units of 2-bromomethyl acrylates afforded polyalkenyl adducts containing two cyclohexenyl rings. This reaction occurs under mild conditions providing the final product by formation of seven carbon–carbon bonds and four stereocenters. Experimental and computational studies support an initial dimerization of the substrate, which in turn trimerizes involving two totally regio- and stereocontrolled Diels–Alder cycloadditions. The yield of the hexamerization of the 2-bromomethyl acrylates depends on the size of the ester function. The protocol has also proved to be practicable on a gram scale.



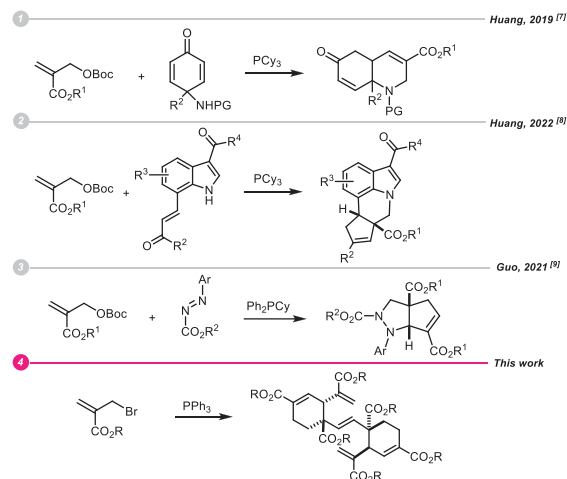
Over the past two decades, nucleophilic phosphine catalysis has emerged as a powerful tool in organic synthesis.¹ Specifically, the initial addition of a tertiary phosphine to an electrophilic π system generates a zwitterionic species that can in turn evolve in different ways, often in cascade processes.^{2–4} In this context, Morita–Baylis–Hillmann (MBH) adducts are very interesting electrophilic partners. Lu and co-workers reported the PPh_3 -catalyzed annulation between 2-halomethyl acrylates and *N*-phenylmaleimide⁵ or tropone, to afford [3 + 3] or [3 + 6] cycloadducts, respectively.⁶ More recently, by using PCy_3 -catalyst, Huang described a [3 + 3] annulation between MBH carbonates and 4-amino-cyclohexandienones (Scheme 1, eq 1)⁷ as well as the sequential [2 + 4]/[2 + 3] annulation between MBH carbonates and 7-alkenyl-indoles (Scheme 1, eq 2).⁸ Finally, Guo discovered a Ph_2PCy catalyzed annulation between diazenes and MBH carbonates (Scheme 1, eq 3).⁹

As part of our ongoing studies on the development of new domino processes,¹⁰ we report on a reaction that generates bicyclic structures through the assembly of six 2-(bromomethyl)acrylate units (Scheme 1, eq 4).

The treatment of methyl 2-(bromomethyl)acrylate (**1a**) with PPh_3 (40 mol %) and triethylamine (1.0 mmol) for 24 h at room temperature afforded the bicyclic structure **2** in 63% yield, as confirmed by a single-crystal X-ray diffraction analysis (Scheme 2).

Such a striking totally regio- and stereoselective hexamerization involving the generation of seven C–C bonds and the control of four stereocenters prompted us to further investigate this reactivity. By extending the reaction time to 72 h, the yield was increased to 81% (Table 1, entry 1). By increasing the reaction temperature to 40 °C for 7 h or using 1.0 mmol of

Scheme 1. Selected Phosphine-Mediated Reactions Involving MBH Adducts or Derivatives

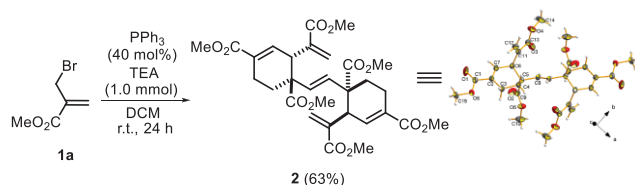


PPh_3 for 24 h did not improve the yield (Table 1, entries 2, 3). Conversely, the use of a catalytic amount of PPh_3 (10 mol %) gave only traces of the pentaenic product and a complex mixture of degradation products (Table 1, entry 4). The use of

Received: September 2, 2023

Published: September 29, 2023



Scheme 2. PPh₃-Catalyzed Hexamerization of Methyl 2-(Bromomethyl)acrylate^{a,b,c}


^aReaction conditions: methyl acrylate (1.0 mmol), PPh₃ (0.4 mmol), TEA (1.0 mmol), DCM (0.1 M), r.t., 24 h. ^bIsolation yields. ^cCCDC 2286203 is the Cambridge Structural Database entry for 2.

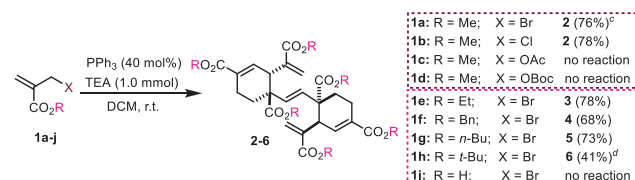
Table 1. Phosphine-Catalyzed Hexamerization of Methyl 2-(Bromomethyl)acrylate to 2

entry ^a	PR ₃	base	temp (°C)	2 (%) ^b
1 ^c	PPh ₃	TEA	r.t.	81
2 ^d	PPh ₃	TEA	40	77
3 ^e	PPh ₃	TEA	r.t.	71
4 ^f	PPh ₃	TEA	r.t.	traces
5	PPh ₃	DIPEA	r.t.	56
6	PPh ₃	Na ₂ CO ₃	r.t.	degrad.
7	PPh ₃	K ₂ CO ₃	r.t.	degrad.
8	PCy ₃	TEA	r.t.	degrad.
9	PBu ₃ ^g	TEA	r.t.	degrad.
10	Johnphos	TEA	r.t.	degrad.
11	(2-Furyl) ₃ P	TEA	r.t.	69
12	BINAP	TEA	r.t.	traces
13	BINAP	TEA	40	26

^aReaction conditions: 1a (1.0 mmol), phosphine (40 mol %), base (1.0 mmol), DCM (0.1 M), 24 h. ^bIsolation yields. ^cReaction time: 72 h. ^dReaction time: 7 h. ^ePPh₃ (1.0 mmol). ^fPPh₃ (10 mol %).

DIPEA, Na₂CO₃, or K₂CO₃ as bases, instead of TEA, led to unsatisfactory results (Table 1, entries 5–7). Replacing PPh₃ with Cy₃P, *n*Bu₃P, or JohnPhos furnished only tarry products (Table 1, entries 8–10). On the other hand, the use of tri-2-furylphosphine led to 2 in 69% yield (Table 1, entry 11). The use of (±)-BINAP gave only traces of 2 at r.t., while heating the mixture at 40 °C allowed only a moderate yield improvement (Table 1, entries 12 and 13).

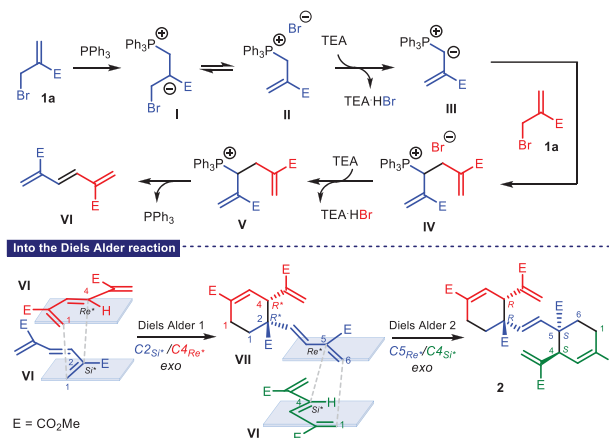
A set of additional experiments completed our initial study (Scheme 3). The hexamerization process also took place from methyl 2-chloromethyl acrylate 1b, providing 2 in 78% yield. Conversely, the corresponding MBH acetate or carbonate was not reactive. Finally, repetition of the hexamerization of 1a on a 3.0 mmol scale gave 2 in 76% yield after a 120 h reaction.

Scheme 3. PPh₃-Catalyzed Hexamerization of Differently Substituted Acrylates^{a,b}


^aReaction conditions: acrylates 1b–j (1.0 mmol), PPh₃ (0.4 mmol), TEA (1.0 mmol), DCM (0.1 M), r.t., 72 h. ^bIsolation yields. ^cGram scale reaction: 1a (3.0 mmol), PPh₃ (1.2 mmol), TEA (3.0 mmol), DCM (0.1 M), r.t., 5 days. ^d5 days.

Different MBH esters were next tested to check the scope of this new phosphine-catalyzed cascade reaction. Accordingly, ethyl, benzyl, *n*-butyl, and *tert*-butyl 2-(bromomethyl)acrylates (1e–h) smoothly afforded the corresponding pentaenic bicyclic structures 3–6 in variable yields depending on the steric hindrance of the ester. Conversely, 2-(bromomethyl)acrylic acid, 2-(bromomethyl)acryl *N,N*-dimethylamide, and the simple allyl bromide failed in the phosphine-catalyzed assembly.

A possible reaction mechanism is proposed in Scheme 4 for compound 2. Conjugate addition of triphenylphosphine to 2-

Scheme 4. Proposed Mechanism for the Conversion of 2-(Bromomethyl)acrylate 1a into Dicyclohexenyl Product 2


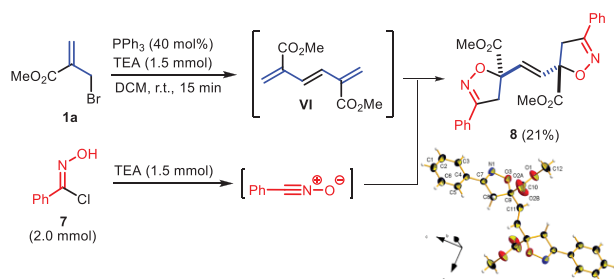
(bromomethyl)acrylate followed by bromide elimination generates phosphonium bromide II via I, which, in the presence of triethylamine, gives the corresponding ylide III. A second conjugate addition/elimination sequence takes place between III and a new unit of acrylate to generate adduct IV. Subsequent deprotonation of IV by triethylamine triggers triphenylphosphine elimination with generation of conjugated triene VI via V. However, as the most acidic H atom in IV is on the carbon atom directly linked to the phosphorus atom, the generation of V may pass through the reversible formation of an unproductive ylide (not shown), or ylide formation is followed by a 1,2 proton shift.

From this point, the generation of pentaenic product 2 appears to derive from two consecutive Diels–Alder (DA) cycloadditions involving three units of key triene VI. In particular, while two units of VI act as dienes, the third one plays the role of a double dienophile. The formation of 2 as single regio- and stereoisomer of *C_i* point group symmetry implies that an *exo*-control (C2 dienophile/C4 diene *Si**/*Re**) is at work during the first cycloaddition to give intermediate VII, while an opposite *exo*-control (C5 dienophile/C4 diene *Re**/*Si**) takes place in the second cycloaddition. This means that besides the regioselectivity, a total diastereoselectivity is at work in both of the cycloadditions.

Since the proposed mechanism is based on the involvement of triene VI, it was essential to prove the formation of this key intermediate. Despite several trials, detection of VI in crude reaction mixtures, even after short reaction times, was fruitless. Hence, indirect detection of VI was planned. We chose a nitrile oxide as a trapping agent, as this 1,3-dipole is known to regioselectively react with electron-poor dipolarophiles.¹¹ After a 15 min exposure of 2-(bromomethyl)acrylate to triphenyl-

phosphine and triethylamine, the addition of chloroxime **7** and triethylamine (to generate benzonitrile oxide) afforded the centrosymmetric bis-isoxazoline **8** as the sole product (Scheme 5). Again, the double cycloaddition was totally regio- and stereoselective, as confirmed by X-ray diffraction analysis of a single crystal of **8**.

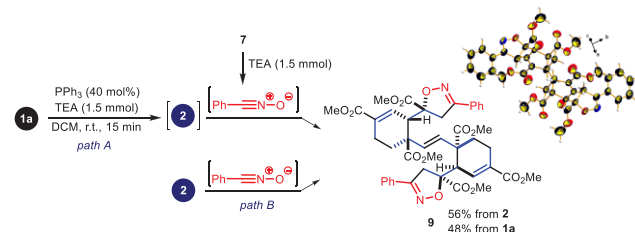
Scheme 5. Capture of Triene Intermediate by 1,3-Dipolar Cycloaddition^{a,b,c}



^aReaction conditions: step 1: **1a** (1.0 mmol), PPh₃ (0.4 mmol), TEA (1.5 mmol), DCM (0.1 M), r.t., 15 min.; step 2: **7** (2.0 mmol), TEA (1.5 mmol), r.t., 24 h. ^bIsolation yields. ^cCCDC 2286201 is the Cambridge Structural Database entry for **8**.

Given the presence of five ethylenic bonds in **2**, we considered its functionalization via 1,3-dipolar cycloaddition to increase the molecular complexity. Accordingly, treatment of **2** with benzonitrile oxide (*in situ* generated from **7** and TEA) afforded the tetracyclic centrosymmetric bis-isoxazole **9** in 56% yield as the sole product, whose structure was confirmed by X-ray diffraction analysis (Scheme 6, path B). So, once again, the

Scheme 6. Dimerization/Diels–Alder/1,3-Dipolar Cycloadditions from **1a**^{a,b,c}



^aReaction conditions: path A: **1a** (1.0 mmol), PPh₃ (0.4 mmol), DCM (0.1 M), r.t., 72 h; then: **7** (2.0 mmol), TEA (1.5 mmol), r.t., 24 h; path B: **2** (1.0 mmol), **7** (2.0 mmol), TEA (1.5 mmol), DCM (0.1 M), r.t., 24 h. ^bIsolation yields. ^cCCDC 2286202 is the Cambridge Structural Database entry for **9**.

reaction was totally regio- and stereoselective. Compound **9** could also be obtained in good yield (48%) in a *one-pot* process by generating *in situ* benzonitrile oxide in the presence of **2**, which was in turn *in situ* generated from **1a**, providing on the whole a dimerization/double DA cycloaddition/double 1,3-dipolar cycloaddition process (Scheme 6, path A).

To understand the reason for such a total stereoselectivity, DFT calculations were performed.^{12,13} The lowest energy geometry (Table S1, Supporting Information (SI)) for each ground state and transition state (TS) was used for evaluating the enthalpy (Figure 1A and B) and free energy (Figure S1A and B; SI) paths of the first and second cycloaddition. As to the first cycloaddition, we modeled the reaction between two

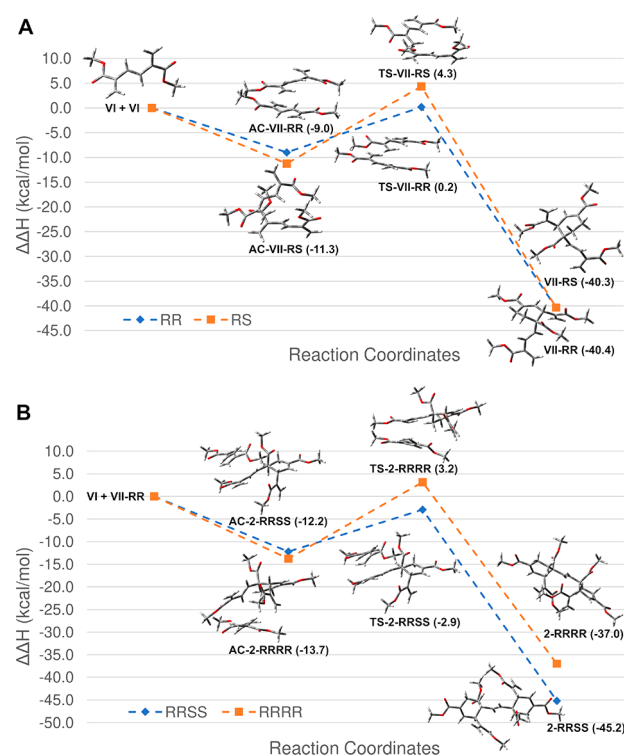


Figure 1. DFT and QTAIM analysis of the reaction mechanism leading to experimentally isolated and nonisolated stereoisomers. (A) Enthalpy path and stationary points for the dimerization of **VI**, leading to **VII-RS** and **VII-RR**. (B) Enthalpy path and stationary points for the addition of **VII-RR** to **VI**, leading to **2-RRRR** (not isolated) and **2-RRSS** (isolated) stereoisomers. ΔH values relative to the isolated reactants are reported in parentheses in kcal/mol.

molecules of monomer **VI** to provide intermediate **VII** in both the 3*R*,4*R* (**VII-RR**) and 3*R*,4*S* (**VII-RS**) stereochemistries. We found that the path leading to the former stereoisomer was kinetically favored over the second, with activation barriers (ΔH^\ddagger) = 9.2 and 15.6 kcal/mol, respectively, from the activated complex (AC-**VII** vs TS-**VII**). No relevant difference was found in reaction enthalpy (ΔH), suggesting that **VII-RR** and **VII-RS** are thermodynamically equivalent (Figure 1A). As to the second cycloaddition, we investigated the reaction between the kinetically favored **VII-RR** and monomer **VI**, leading to the **2-RRSS** and **2-RRRR** diastereoisomers (Figure 1B). In this case, the former compound was favored over **2-RRRR** both kinetically (ΔH^\ddagger = 9.3 and 16.9 kcal/mol, respectively; AC-**2** vs TS-**2**) and thermodynamically (ΔH = -33.0 and -23.3 kcal/mol, respectively; **2** vs AC-**2**).

We analyzed the difference between TS-**2-RRSS** and TS-**2-RRRR** by performing a topological analysis of the electron density using the Bader's Quantum Theory of Atoms in Molecules (QTAIM).^{14,15} In QTAIM, both covalent and noncovalent interactions are defined by a bond path (BP) and by a bond critical point (BCP). The value of electron density $\rho(r)$ at the BCP is a measure of the strength of the interaction. Results are summarized in Figure S2A, B (SI) and Table S2 (SI), where BPs connecting noncovalently bound oxygen and hydrogens (HB) are reported with the corresponding BCPs. From the molecular graphs, it can be observed that four HB BCPs (BCP1–4) are found for TS-**2-RRRR** (Figure S2A, SI), three of which belong to intermolecular BPs connecting the two reactants. Conversely, eight HB BCPs were found in TS-**2-**

RRSS, six of which were intermolecular. Additionally, the total electron density $\rho(r)$ of HB BCPs is 0.066659 and 0.047609 au for TS-2-RRSS and TS-2-RRRR, respectively. This indicates stronger, as well as more numerically abundant, interactions among the reactants in the former TS, justifying the selectivity observed both theoretically and experimentally.

In conclusion, we have disclosed a highly effective phosphine-catalyzed procedure that allows assembly, in a totally regio- and stereoselective way, of six molecules of 2-(bromomethyl)acrylates through the formation of seven carbon-carbon bonds and four stereocenters. The resulting sole product is a centrosymmetric pentaene containing two cyclohexenyl units derived from a dimerization/double DA cycloaddition sequence. A key intermediate of this domino sequence is the 2,5-dicarbomethoxy-1,3,5-triene VI, whose formation was evidenced by its trapping through a 1,3-dipolar cycloaddition with benzonitrile oxide. Furthermore, adduct 2 was also found to undergo a double and totally selective 1,3-dipolar cycloaddition with benzonitrile oxide, generating a tetracyclic bis-isoxazole adduct as the sole product. DFT computations of the two DA steps supported the proposed mechanism. Computed ΔH^\ddagger are consistent with a reaction occurring at room temperature as well as with the observed selectivity. Future studies will be directed toward expanding the scope of the reaction between 1 and other 1,3-dipoles to achieve new structures and higher complexity.

■ ASSOCIATED CONTENT

Data Availability Statement

The data underlying this study are available in the published article and its [Supporting Information](#).

Supporting Information

The Supporting Information is available free of charge at <https://pubs.acs.org/doi/10.1021/acs.orglett.3c02836>.

Experimental procedures, compound characterization data including copies of ^1H and ^{13}C NMR spectra, computational details, and crystallographic data for compounds 2, 8, and 9. (PDF)

Accession Codes

CCDC 2286201–2286203 contain the supplementary crystallographic data for this paper. These data can be obtained free of charge via www.ccdc.cam.ac.uk/data_request/cif, or by emailing data_request@ccdc.cam.ac.uk, or by contacting The Cambridge Crystallographic Data Centre, 12 Union Road, Cambridge CB2 1EZ, UK; fax: +44 1223 336033.

■ AUTHOR INFORMATION

Corresponding Author

Camilla Loro – Dipartimento di Scienza e Alta Tecnologia, Università degli Studi dell'Insubria, 22100 Como, Italy; orcid.org/0000-0001-9616-2335; Email: camilla.loro@uninsubria.it

Authors

Marta Papis – Dipartimento di Scienza e Alta Tecnologia, Università degli Studi dell'Insubria, 22100 Como, Italy
Raffaella Bucci – Dipartimento di Scienze Farmaceutiche, DISFARM Università degli Studi di Milano, 20133 Milano, Italy; orcid.org/0000-0002-5465-9447

Alessandro Contini – Dipartimento di Scienze Farmaceutiche, DISFARM Università degli Studi di Milano, 20133 Milano, Italy; orcid.org/0000-0002-4394-8956

Maria Luisa Gelmi – Dipartimento di Scienze Farmaceutiche, DISFARM Università degli Studi di Milano, 20133 Milano, Italy; orcid.org/0000-0003-0743-5499

Leonardo Lo Presti – Dipartimento di Chimica, Università degli Studi di Milano, 20133 Milano, Italy; orcid.org/0000-0001-6361-477X

Giovanni Poli – Sorbonne Université, Faculté des Sciences et Ingénierie, CNRS, Institut Parisien de Chimie Moléculaire, IPCM, 75005 Paris, France; orcid.org/0000-0002-7356-1568

Gianluigi Brogгинi – Dipartimento di Scienza e Alta Tecnologia, Università degli Studi dell'Insubria, 22100 Como, Italy; orcid.org/0000-0003-2492-5078

Complete contact information is available at: <https://pubs.acs.org/10.1021/acs.orglett.3c02836>

Notes

The authors declare no competing financial interest.

■ ACKNOWLEDGMENTS

Università dell'Insubria is gratefully acknowledged for financial support by C.L., M.P., and G.B. G.P. acknowledges support by Sorbonne Université and CNRS. A.C., R.B., M.L.G., and L.L.P. thank Università di Milano for financial support.

■ REFERENCES

- (1) (a) Khong, S.; Venkatesh, T.; Kwon, O. Nucleophilic Phosphine Catalysis: The Untold Story. *Asian J. Org. Chem.* **2021**, *10*, 2699–2708. (b) Xie, C.; Smaligo, A. J.; Song, X.-R.; Kwon, O. Phosphorus-Based Catalysis. *ACS Cent. Sci.* **2021**, *7*, 536–558. (c) Guo, H.; Fan, C. Y.; Sun, Z.; Wu, Y.; Kwon, O. Phosphine Organocatalysis. *Chem. Rev.* **2018**, *118*, 10049–10293. (d) Ni, H.; Chan, W.-L.; Lu, Y. Phosphine-Catalyzed Asymmetric Organic Reactions. *Chem. Rev.* **2018**, *118*, 9344–94. (e) Methot, J. L.; Roush, W. R. Nucleophilic Phosphine Organocatalysis. *Adv. Synth. Catal.* **2004**, *346*, 1035–1050.
- (2) (a) Pitchumani, V.; Breugst, M.; Lupton, D. W. Enantioselective Rauhut-Currier Reaction with β -Substituted Acrylamides Catalyzed by *N*-Heterocyclic Carbenes. *Org. Lett.* **2021**, *23*, 9413–9418. (b) Vagh, S. S.; Hou, B.-J.; Edukondalu, A.; Wang, P.-C.; Chen, Y.-R.; Lin, W. Phosphine-Mediated Rauhut-Currier-Type/Acyl Transfer/Wittig Strategy for Synthesis of Spirocyclopenta[*c*]chromene-Indolinones. *Adv. Synth. Catal.* **2021**, *363*, 5429–5435. (c) Xiao, B.-X.; Jiang, B.; Song, X.; Du, W.; Chen, Y.-C. Phosphine-catalysed asymmetric dearomative formal [4 + 2] cycloadditions of 3-benzofuranyl vinyl ketones. *Chem. Commun.* **2019**, *55*, 3097–3100.
- (3) (a) Zhang, K.; Cai, L.; Yang, Z.; Houk, K. N.; Kwon, O. Bridged [2.2.1] bicyclic phosphine oxide facilitates catalytic γ -umpolung addition-Wittig olefination. *Chem. Sci.* **2018**, *9*, 1867–1872. (b) Oda, R.; Kawabata, T.; Tanimoto, S. Entsehung von P-Ylid aus Triphenylphosphin und Acrylsäurederivaten. *Tetrahedron Lett.* **1964**, *5*, 1653–1657.
- (4) (a) Zhang, Q.; Zhu, Y.; Jin, H.; Huang, Y. A phosphine mediated sequential annulation process of 2-tosylaminochalcones with MBH carbonates to constructs functionalized aza-benzobicyclo[4.3.0] derivatives. *Chem. Commun.* **2017**, *53*, 3974–3977. (b) Xie, P.; Huang, Y. Morita-Baylis-Hillman adduct derivatives (MBHADs): versatile reactivity in Lewis base-promoted annulation. *Org. Biomol. Chem.* **2015**, *13*, 8578–8595. (c) Wei, Y.; Shi, M. Recent Advances in Organocatalytic Asymmetric Morita-Baylis-Hillman/aza-Morita-Baylis-Hillman Reactions. *Chem. Rev.* **2013**, *113*, 6659–6690. (d) Zhang, X.; Deng, H.-P.; Huang, L.; Wei, Y.; Shi, M. Phosphine-catalyzed

asymmetric [4 + 1] annulation of Morita-Baylis-Hillman carbonates with dicyano-2-methylenebut-3-enoates. *Chem. Commun.* **2012**, 48, 8664–8666. (e) Song, H.-L.; Yuan, K.; Wu, X.-Y. Chiral phosphine-squaramides as enantioselective catalysts for the intramolecular Morita-Baylis-Hillman reaction. *Chem. Commun.* **2011**, 47, 1012–1014. (f) Deng, H.-P.; Wei, Y.; Shi, M. Highly Regio- and Diastereoselective Construction of Spirocyclopenteneoxindoles through Phosphine-Catalyzed [3 + 2] Annulation of Morita-Baylis-Hillman Carbonates with Isatylidene Malononitriles. *Org. Lett.* **2011**, 13, 3348–3351.

(5) Du, Y.; Lu, X.; Zhang, C. A Catalytic Carbon-Phosphorus Ylide Reaction: Phosphane-Catalyzed Annulation of Allylic Compounds with Electron-Deficient Alkenes. *Angew. Chem., Int. Ed.* **2003**, 42, 1035–1037.

(6) Du, Y.; Feng, J.; Lu, X. A Phosphine-Catalyzed [3 + 6] Annulation Reaction of Modified Allylic Compounds and Tropone. *Org. Lett.* **2005**, 7, 1987–1989.

(7) Jin, H.; Lai, J.; Huang, Y. Phosphine-Catalyzed Domino [3 + 3] Cyclization of *para*-Quinamines with Morita-Baylis-Hillman Carbonates: Access to Hydroquinoline Derivatives. *Org. Lett.* **2019**, 21, 2843–2846.

(8) Lin, J.; Zhu, Y.; Cai, W.; Huang, Y. Phosphine-Mediate Sequential [2 + 4]/[2 + 3] Annulation to Construct Pyrroloquinolines. *Org. Lett.* **2022**, 24, 1593–1597.

(9) Li, H.; Shi, W.; Wang, C.; Liu, H.; Wang, W.; Wu, Y.; Guo, H. Phosphine-Catalyzed Cascade Annulation of MBH Carbonates and Diazenes: Synthesis of Hexahydrocyclopenta[*c*]pyrazole Derivatives. *Org. Lett.* **2021**, 23, 5571–5575.

(10) (a) Loro, C.; Molteni, L.; Papis, M.; Beccalli, E. M.; Nava, D.; Presti, L. L.; Brenna, S.; Colombo, G.; Foschi, F.; Broggin, G. Direct Synthesis of Fluorescent Oxazolo-phenoxazine by Copper-Catalyzed/Hypervalent Iodine(III)-Mediated Dimerization/Cyclization of 2-Benzylamino-phenols. *J. Org. Chem.* **2022**, 87, 1032–1042. (b) Loro, C.; Oble, J.; Foschi, F.; Papis, M.; Beccalli, E. M.; Giofrè, S.; Poli, G.; Broggin, G. Acid-mediated decarboxylative C-H coupling between arenes and *O*-allyl carbamates. *Org. Chem. Front.* **2022**, 9, 1711–1718. (c) Giofrè, S.; Loro, C.; Molteni, L.; Castellano, C.; Contini, A.; Nava, D.; Broggin, G.; Beccalli, E. M. Copper(II)-Catalyzed Amino-halogenation of Alkynyl Carbamates. *Eur. J. Org. Chem.* **2021**, 2021, 1750–1757. (d) Foschi, F.; Loro, C.; Sala, R.; Oble, J.; Lo Presti, L.; Beccalli, E. M.; Poli, G.; Broggin, G. Intramolecular Aminoazidation of Unactivated Terminal Alkenes by Palladium-Catalyzed Reactions with Hydrogen Peroxide as the Oxidant. *Org. Lett.* **2020**, 22, 1402–1406.

(11) (11) Buccì, R.; Vaghi, F.; Di Lorenzo, D.; Anastasi, F.; Broggin, G.; Lo Presti, L.; Contini, A.; Gelmi, M. L. A Non-coded $\beta^{2,2}$ -Amino Acid with Isoxazoline Core Able to Stabilized Peptides Folding through an Unprecedented Hydrogen Bond. *Eur. J. Org. Chem.* **2022**, 2022, No. e202200601.

(12) Each ground state geometry was subjected to a molecular mechanics conformational search (MMFF94x force field, born solvation model for DCM). Conformations within 1.5 kcal/mol were reoptimized by DFT at the ω B97X-D/6-311++G(3df,3pd)// ω B97X-D/6-31+G(d, p) level. Solvation was considered using the CPCM model for DCM in single point energy calculations. See SI for additional details.

(13) Mardirossian, N.; Head-Gordon, M. Thirty years of density functional theory in computational chemistry: an overview and extensive assessment of 200 density functionals. *Mol. Phys.* **2017**, 115, 2315–2372.

(14) (a) Lu, T.; Chen, F. Multiwfn: A multifunctional wavefunction analyzer. *J. Comput. Chem.* **2012**, 33, 580–592. (b) Bader, R. F. W. Atoms in Molecules: a Quantum Theory. *International Series of Monographs on Chemistry* 22; Oxford University Press: Oxford, 1990.

(15) (a) Maffucci, I.; Pellegrino, S.; Clayden, J.; Contini, A. Mechanism of Stabilization of Helix Secondary Structure by Constrained α -Tetrasubstituted α -Amino Acids. *J. Phys. Chem. B* **2015**, 119, 1350–1361. (b) Maffucci, I.; Clayden, J.; Contini, A. Origin of Helical Screw Sense Selectivity Induced by Chiral

Constrained α -Tetrasubstituted α -Amino Acids in Aib-based Peptides. *J. Phys. Chem. B* **2015**, 119, 14003–14013. (c) Contini, A.; Erba, E. Click-chemistry approach to azacycloalkene monosulfonyl diamines: synthesis and computational analysis of the reaction mechanism. *RSC Adv.* **2012**, 2, 10652–10660.